JOHANNES KEPLER
UNIVERSITÄT LINZ

Author
Vilja Langer

Submission
Institute for Analytical and General Chemistry

Thesis Supervisor
Laura Zellner, MSc

July 2024

UPTAKE AND METABOLISM OF KETAMINE AND PARACETAMOL IN GARDEN CRESS

Bachelor's Thesis

to confer the academic degree of

Bachelor of Science

in the bachelor's program

Biological Chemistry

JOHANNES KEPLER
UNIVERSITÄT LINZ
Altenberger Straße 69
4040 Linz, Österreich
www.jku.at

Table of Contents

Abstract

The escalating effects of global warming are causing severe water shortages worldwide, leading to increased use of wastewater for agricultural irrigation processes. This practice carries potential risks due to the tentative presence of various contaminants, such as pharmaceuticals, as these might be taken up by plants.

This research aims to investigate the absorption rate of two pharmaceuticals, paracetamol and ketamine, in garden cress (*Lepidium sativum*) under hydroponic conditions. The absorbed pharmaceuticals are quantified in the root and leaf tissue of garden cress using high-performance liquid chromatography (HPLC) coupled with a quadrupole time-of-flight (QTOF) mass spectrometer. The findings show that varying amounts of both drugs are absorbed, suggesting a potential accumulation of harmful substances within edible crops.

While this study provides preliminary observations, further research is needed to assess long-term effects on plant physiology and to explore the potential for bioaccumulation in different parts of various plant species. The health implications for animals and humans who may consume the polluted crops might require additional investigations. Overall, this study emphasises the importance of proper wastewater treatment to effectively remove pharmaceuticals before irrigation.

1. Introduction

Global warming, driven by the increasing greenhouse gas emissions, influences water resources worldwide. Rising global temperatures accelerate water evaporation from soil and water at an alarming rate, significantly reducing water availability. Additionally, the higher temperatures can lead to a localised reduction in precipitation. With that, the drastic changes in our climate contribute to severe droughts and, subsequently, water scarcity [1].

1.1 Water consumption in agriculture

The overall decline in global water availability necessitates new approaches for water-dependent sectors such as agriculture. From the years 2000 to 2019, in the European Union alone, agriculture accounted for 28 % of the total water abstraction from natural sources, according to the European Environment Agency, making it the second-largest water-consuming sector following electricity production. In China, known for having one of the largest populations globally, the water demand for agricultural use can reach nearly 50 % [2], mirroring global patterns where agriculture persists as a primary user of our water sources. On a global scale, approximately 70 % of the planet's freshwater is used in the agricultural sector, according to the International Atomic Energy Agency, which highlights the vital importance of finding sustainable water management practices. To combat this, the utilisation of wastewater for the irrigation of crops has started to emerge as an agricultural practice [3]. However, this practice brings concerns about introducing pollutants, including xenobiotics, which are not entirely removed in wastewater treatment plants and might be absorbed by agricultural plants and ultimately ingested by human consumers.

1.2 Wastewater and pollutant uptake by crops

Water uptake is a crucial process in the life cycle of crops, playing an essential role in their growth and development. Crops absorb water through their roots, transporting it to their stems, leaves, and flowers. The ability of crops to absorb water from the soil is fundamental for photosynthesis, nutrient transport, and overall plant health [4]. The quality of the available water directly influences the efficiency of this water uptake. The usage of wastewater comes with potential health risks as it may contain pathogens, drugs, toxic chemicals and heavy metals, which can accumulate over time, primarily due to the wastewater discharge from industries [5].

Several studies have linked contaminants to suboptimal crop growth and the accumulation of pollutants in the plans themselves. For instance, one study found that plants absorbed heavy metals - such as lead, manganese, cadmium and chromium - from wastewater, which were detected in different parts of the plants. These findings also showed that tested plants experienced a physiological decline with increasing concentrations of contaminants [6]. Another study found that arsenic in irrigation water limited crop growth in rice, with increasing contaminant concentration leading to more heavy metal accumulation in different parts of the rice plants [7]. In addition to the presence of heavy metals, the increasing discharge of pharmaceuticals into our wastewater can pose a potential risk hazard. For example, it was demonstrated that lettuce takes up several pharmaceuticals, namely anticonvulsants and caffeine, from the used water solution, with higher concentrations found in its shoot, which would be the part of the plant that is consumed by humans [8].

Therefore, ensuring the availability of clean water for agriculture is crucial for sustainable crop production. Clean irrigation water supports the health of crops, the quality of the produce, and, ultimately, the consumers' health.

1.3 Pharmaceutical contaminants

Active pharmaceutical ingredients (APIs), the active component of a medication, could pose potential risks to the health of vegetation, animals and even humans when present in the wastewater. These compounds and their metabolites can rapidly make their way into our environment through several pathways because they are increasingly used in both human and veterinary medicine. The discharge pathways of such chemicals include improper disposal of polluted water during drug manufacturing [9] or following regular therapeutic use, they are excreted into the wastewater [10]. Pharmaceuticals have been found in effluents from sewage treatment plants, as well as in surface water, seawater, groundwater, soil, sediment, and even in aquatic organisms such as fish [11].

1.3.1 Detoxification pathways in plants

Upon absorbing xenobiotics - such as APIs from irrigation water – the plants try to mitigate these foreign chemicals using their detoxification pathway. The absorbed xenobiotics and their metabolites undergo primary transformation through oxidation, reduction or hydrolysis to enhance their reactivity. This is followed by a condensation reaction with endogenous molecules like malonic acid or glucose with the primary goal of increasing the polarity of the xenobiotics. These conjugated compounds, which are more soluble and less cytotoxic, are

usually stored in the vacuoles of the plants [12]. Due to this detoxification pathway, the absorbed xenobiotics and their metabolites might also be present in their conjugated forms inside the plant cells.

1.3.2 Paracetamol

Paracetamol, also known as acetaminophen, is called N-(4-hydroxyphenyl)acetamide in accordance with IUPAC nomenclature. It is a white crystalline powder commonly used for mild to moderate pain and fever [13]. Paracetamol can be found in its pure form under various brand names for oral consumption. Additionally, it is included in combined drug preparations [14]. The molecular structure of paracetamol is depicted in *Figure 1*, and its basic physical and chemical properties are summarised in *Table 1*.

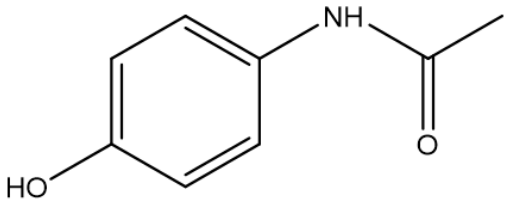

Figure 1 – Molecular structure of paracetamol

Table 1 - Chemical and physical properties of paracetamol [15]

Parameter	**Value**
Sum formula	$C_8H_9NO_2$
Molecular weight / g mol^{-1}	151.16
Monoisotopic mass / u	151.0633
Melting point / °C	169-171
Solubility / g L^{-1}	14
pK_a	9.46
logP	0.46
Physiological charge	0

Followed by oral consumption, paracetamol is mainly metabolised by the liver and, to a lesser degree, also by the kidneys [16]. The main metabolic pathways and the subsequent by-products produced in the liver are described in *Figure 2*.

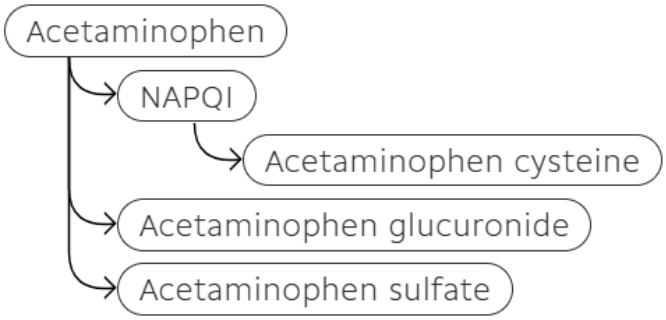

Figure 2 - Paracetamol metabolites in the human liver cells [17]

1.3.3 Ketamine

Ketamine is called 2-(2-chlorophenyl)-2-(methylamino)cyclohexan-1-one according to IUPAC nomenclature. Although it is a white powder in its pure state, it is commonly utilised in a liquid form due to its solubility in water as a hydrochloride salt. Ideally, it is administered intravenously; however, this method is not always possible, and therefore, other ways, such as intramuscular injection, are also common [18]. The S(+) enantiomer of ketamine, called eskatemine or S(+)-ketamine, is the configuration that is used as the API [19]. This drug is used for managing more severe pain, as an antidepressant and as an anaesthetic [20]. *Figure 3* demonstrates the molecular structure S(+)-ketamine and *Table 2* presents its general physical and chemical properties.

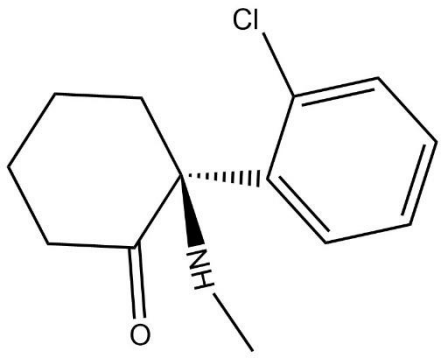

Figure 3 – Molecular structure of S(+)-ketamine

Table 2 – Chemical and physical properties of ketamine [21]

Parameter	**Value**
Sum formula	$C_{13}H_{16}ClNO$
Molecular weight / g mol^{-1}	237.725
Monoisotopic mass / u	237.092
Melting point / °C	92-93
Solubility / g L^{-1}	0.0464
pK_a	18.78
logP	2.9
Physiological charge	1

The possible metabolic pathways of ketamine are summarised in *Figure 4.* It is primarily metabolised in liver cells, predominantly through the N-demethylation pathway, which leads to the production of the metabolite norketamine [22].

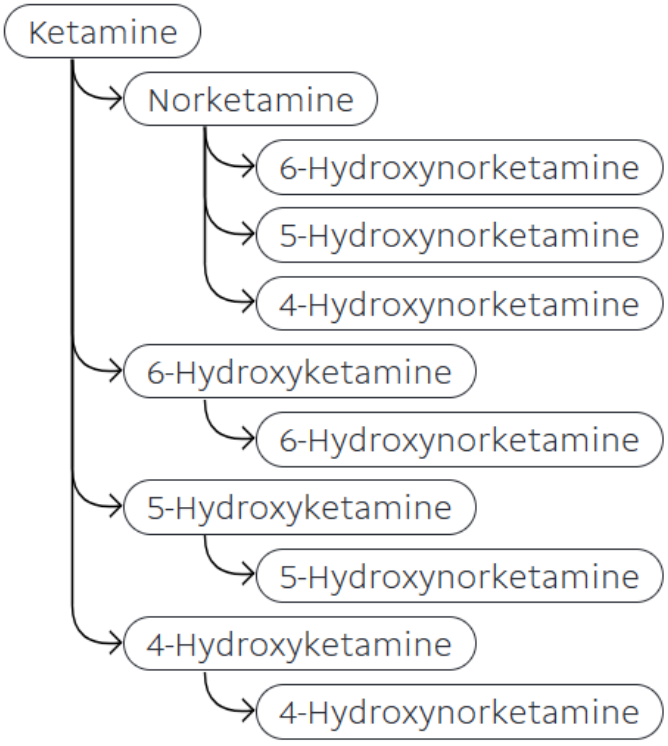

Figure 4 - Ketamine metabolites produced by human liver cells [23]

2. Research objectives

This research project aims to investigate the absorption rate of xenobiotics - specifically paracetamol and ketamine - from drug-spiked water by cress plants. The primary goal of this study is to quantify the concentrations of these APIs in the plant roots and leaves. This will provide a deeper insight into the extent to which the plants absorb and accumulate xenobiotics from the irrigation water, highlighting potential impact on plant, animal and human health. In addition, this research also seeks to examine whether the chosen plant transforms these compounds into different metabolites, which can improve the understanding of the metabolic capabilities of plants.

Furthermore, the study also focuses on the effectiveness of two distinct extraction methods. The first approach involves mechanical extraction with a ball mill, while the second process employs manual extraction by grinding using a mortar and a pestle.

To achieve these goals, the project employs an HPLC QTOF instrument to measure the concentration of paracetamol and ketamine in various parts of the plant.

3. Materials and methods

3.1 Chemicals and materials

HPLC grade chemicals:

- Acetonitrile (ACN; ≥ 99.8 %) from VWR (Vienna, Austria)
- Methanol (MeOH; ≥ 99.8 %) from VWR (Vienna, Austria)
- Hydrochloric acid (HCl; ≥ 37 %) from Sigma Aldrich (Steinheim, Germany)
- Formic acid (FA; ≥ 99.9 %) from Sigma Aldrich (Steinheim, Germany)
- Ultrapure water (Milli-Q®) from Merck Millipore (Bedford, USA)

Analysed pharmaceuticals:

- Paracetamol (≥ 97%) from Sigma Aldrich
- Ketamine (5 mg mL^{-1}) from Pfizer

Additional materials:

- Garden cress (*Lepidium sativum)* seeds
- Conical centrifugation tubes from Greiner Bio-One (Kremsmünster, Austria)
- HPLC vials from Merck (Darmstadt, Germany)
- INOX balls (⌀ 5 mm) from Domel (Železniki, Slovenia)
- Omnifix®- F syringes (1 mL) from B. Braun Melsungen AG (Melsungen, Germany)
- Chromafil® nylon syringe filters (⌀15 mm, pore size: 0.45 µm) from Macherey-Nagel (Düren, Germany)
- Mortar and pestle

3.2 Preparation of standard solutions and irrigation water

For the two APIs to be analysed, two stock solutions with a concentration of 1000 mg L^{-1} were prepared. For this, 10.4 mg of the solid paracetamol was dissolved in pure MeOH to a final volume of 10 mL. The ketamine stock solution was prepared by taking 2 mL of the original ketamine solution from Pfizer (5 mg mL^{-1}) and diluting it with MeOH to a volume of 10 mL.

Both stock solutions were diluted in a dilution series to concentrations of:

- 100 mg L^{-1} (100 µl stock + 900 µL MeOH)
- 10 mg L^{-1} (100 µl 100 mg L^{-1} + 900 µL MeOH)
- 1 mg L^{-1} (100 µl 10 mg L^{-1} + 900 µL MeOH)

- 0.1 mg L^{-1} (100 µl 1 mg L^{-1} + 900 µL Milli-Q® water)
- 0.01 mg L^{-1} (100 µl 0.1 mg L^{-1} + 900 µL Milli-Q® water)
- 0.001 mg L^{-1} (100 µl 0.01 mg L^{-1} + 900 µL Milli-Q® water)

All the prepared solutions, including the stock solutions, were kept in a freezer at - 20 °C until further analysis.

To prepare the irrigation water for the cress plants, the two stock solutions were diluted to a final concentration of 5 mg L^{-1} each. For this, 5 mL of the respective stock solution were diluted with tap water to a final volume of 500 mL. These were then stored in a dark, enclosed cupboard until further use to prevent potential light-induced reactions.

3.3 Laboratory cultivation of garden cress

On the first cultivation day, five batches of garden cress seeds (~ 3 g each) were soaked in tap water for two hours before spreading them on the grids of the cultivation sets. One batch was irrigated solely with tap water, serving as the negative control. Two batches were watered with the paracetamol irrigation water, and two sets were filled with ketamine irrigation water. The plants were grown under hydroponic conditions on a laboratory bench, and the irrigation water was refilled on the tenth cultivation day. *Figures 5* and *6* show the cress seed batches developing over time.

Figure 5 - The five batches of hydroponically grown cress plants on **cultivation day four.**

Figure 6 - The five batches of hydroponically grown cress plants on **cultivation day ten.**

Additionally, to monitor potential photochemical reactions as well as the hydrolysis of the pharmaceutical compounds, the leftovers of the irrigation water solutions were placed by a window in transparent volumetric flasks.

3.3 Preparation of plant extracts

The plant parts were collected on cultivation days 8, 10, 15 and 18, designated as harvest days 1, 2, 3, and 4, respectively. Approximately 500 mg of roots and 500 mg of leaves were collected on each harvest day in Eppendorf tubes. To remove traces of irrigation water, the roots were washed with tap water and dried with paper towel before weighing. An extra batch of leaves and roots was collected on the second harvest day for the manual extraction method. The plants for the negative control were harvested on harvest day three. *Figures 7* and *8* display the distinctive parts of the cress plant, highlighting the white roots and the upper parts with the green leaves used for the analysis. To increase the efficiency of the extraction process, the harvested plant parts were priorly frozen at -80 °C.

Figures 7,8 – Distinctive **roots** and **leaves** of the cress plant, on cultivation day eighteen (harvest day 4)

For the mechanical solid-liquid extraction, 1.5 mL of the extraction solvent (ACN:0.1 M HCl in a 1:2 ratio) and five grinding balls were added to each Eppendorf tube containing the frozen sample. The mixtures were homogenised in a ball mill grinder at a frequency of 25 Hz for 15 minutes. Following this, the solutions were centrifuged at a speed of 4700 rpm for 8 minutes.

For the manual solid-liquid extraction, the frozen plant material was finely ground using a mortar and a pestle. The ground material was then transferred back into an Eppendorf tube, to which 1.5 mL of the same extraction solvent as in the mechanical extraction was added. The mixtures were shaken on the ball mill grinder machine for fifteen minutes at 25 Hz, without grinding balls, and subsequently centrifuged for 8 minutes at 4700 rpm.

For both extraction methods, the final step included the careful removal of the supernatant with a syringe and their subsequent filtration through the nylon filters into HPLC vials. These vials with the extracted sample solutions were stored at -80 °C until further analysis.

3.4 HPLC - Ion Mobility QTOF LC/MS instrumentation

The plant extracts and the window solutions were analysed with reversed-phase HPLC, employing the 6560 Ion Mobility QTOF LC instrument from Agilent Technologies. For the separation process, a Kinetex® C18 LC column (50 x 3.0 mm, 2.6 µm, 100 Å) was used.

For detection, mass spectrometry was conducted with the instrument 6560 Ion Mobility QTOF MS from Agilent Technologies in QTOF-only mode. This device featured a Dual Jet Stream Electrospray Ionisation source and was operated in positive ion mode. As sheath and drying gas, nitrogen was employed. The detailed MS parameters are summarised in *Table 3.*

Table 3 - MS parameters

Parameter	**Value**
Drying gas temperature /°C	275
Drying gas flow / L min^{-1}	11
Nebuliser / psi	40
Capillary voltage (ESI) / V	4000
Nozzle voltage / V	1000
Fragmentor voltage /V	400
Acquisition rate / spectra s^{-1}	1
mass-to-charge ratio (m/z) range	100 - 1700

The mobile phases for gradient elution were solvent A (water with 0.1 % FA) and solvent B (ACN with 0.1 % FA). The gradient elution profiles for ketamine and paracetamol analysis are detailed in *Tables 4* and *5*, respectively. The flow rate of the mobile phase was programmed to be 0.7 mL min^{-1}, and the column temperature was maintained at 30.0 °C. The injected volumes were set to 20 µL for both the samples and the negative control, while the standards and the window solutions were injected with a volume of 3 µL. Tap water was used as the blank in the analysis. After the experiment runs, the obtained data were processed using the MassHunter Qualitative B.07.00 software from Agilent Technologies.

Table 4 - Mobile phase **gradient** of HPLC for **ketamine** analysis

time / min	**Solvent A / %**	**Solvent B / %**
0.0	95	5
5.0	93	5
11.0	0	100
12.0	0	100
12.1	95	5
14.0	95	5

Table 5 - Mobile phase **gradient** of HPLC for **paracetamol** analysis

time / min	**Solvent A / %**	**Solvent B / %**
0.0	98	2
2.0	98	2
10.0	90	10
11.0	0	100
12.0	95	5
12.1	95	5
14.0	95	5

4. Results

4.1 Ketamine

The external calibration curve for ketamine, seen in *Figure 9*, was constructed based on the extracted ion chromatograms (EICs) of the standard solutions by plotting peak area, *A*, against the concentrations of the solutions, $\beta_{sol.}$. The highest concentration standard solution of 100 mg L^{-1} was not included in the calibration, as it was not measured.

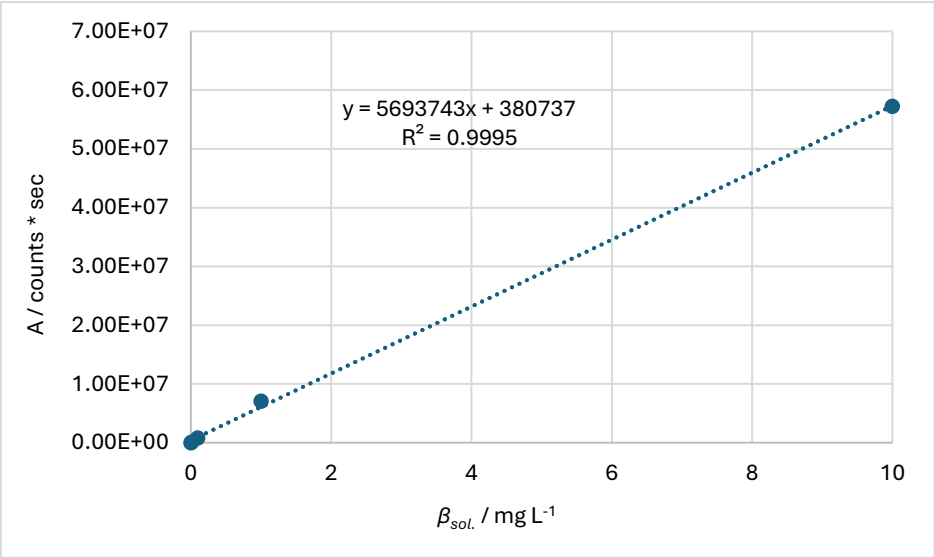

Figure 9 – External calibration curve of ketamine, with **all** the measured **concentrations**

The EICs of the ketamine standard solutions are illustrated in *Figures 10-14*, highlighting the ketamine peaks with a retention time between 5.5 and 5.6 minutes. The peaks are labelled with their areas, marked with an asterisk. The analyte in its protonated form $[M+H]^+$ has an m/z value of 238.0993.

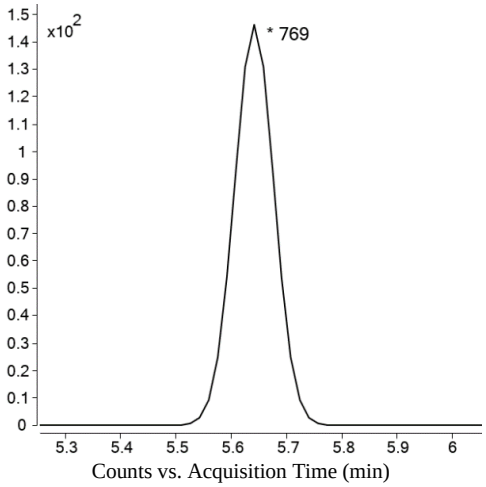

Figure 10 - EIC of **0.001 mg L^{-1}** ketamine

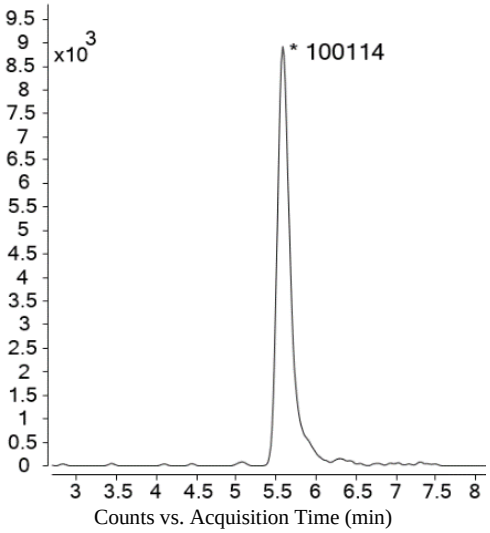

Figure 11 - EIC of **0.01 mg L^{-1}** ketamine

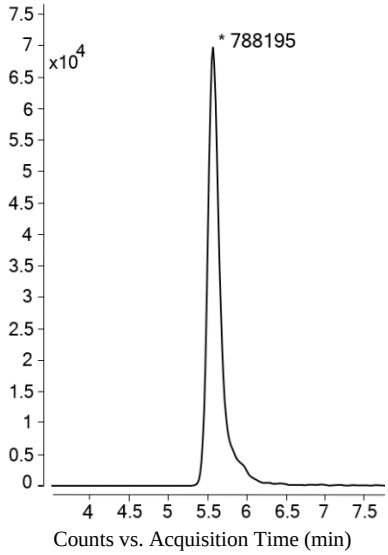

Figure 12 - EIC of **0.01 mg L^{-1}** ketamine

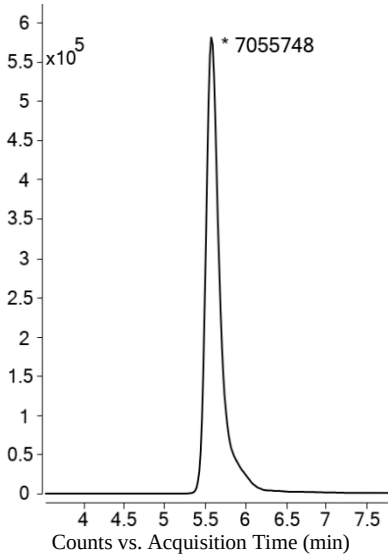

Figure 13 - EIC of **1 mg L^{-1}** ketamine

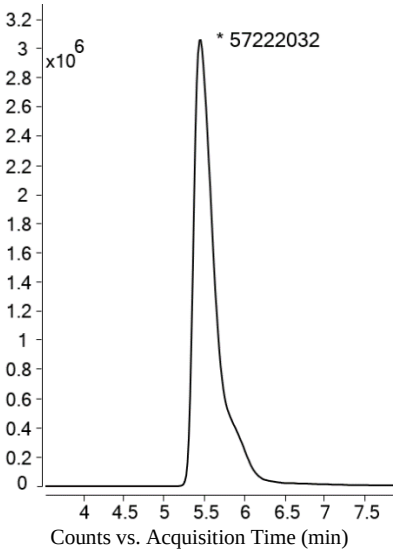

Figure 14 - EIC of **10 mg L^{-1}** ketamine

Since the most prominent peak area of all the tested sample solutions did not exceed the peak area of the 1 mg L^{-1} standard solution, the calibration curve was replotted, excluding the highest concentration and thereby improving the accuracy of the concentration determination. The final external calibration graph and the corresponding equation are shown in *Figure 15*.

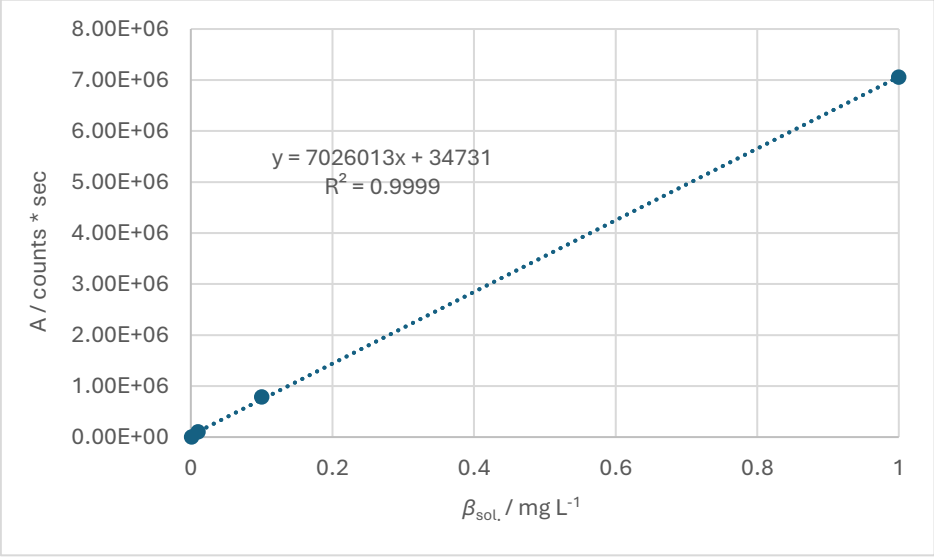

Figure 15 – External calibration curve of ketamine, in the range of **0.001 – 1 mg L^{-1}**

The EICs of the sample solutions were checked for ketamine, its metabolites from *Figure 4*, and their possible conjugates with malonic acid (MA), glucose (Glu) or both. *Table 6* presents an overview of all the examined compounds, listing the m/z values of their protonated forms.

Table 6 – Chemical formulas and the m/z values of the protonated ketamine metabolites, conjugates

Compound	**Chemical formula**	**m/z ($[M+H]^+$)**
Ketamine	$C_{13}H_{16}ClNO$	238.0993
x-Hydroxyketamine	$C_{13}H_{16}ClNO_2$	254.0942
Norketamine	$C_{12}H_{14}ClNO$	224.0837
y-Hydroxynorketamine	$C_{12}H_{14}ClNO_2$	240.0786
Compound with Glu		
Ketamine	$C_{19}H_{26}ClNO_6$	400.1521
x-Hydroxyketamine	$C_{19}H_{26}ClNO_7$	416.1471
Norketamine	$C_{18}H_{24}ClNO_6$	386.1365
y-Hydroxynorketamine	$C_{18}H_{24}ClNO_7$	402.1314
Compound with MA		
Ketamine	$C_{16}H_{18}ClNO_4$	324.1033
x-Hydroxyketamine	$C_{16}H_{18}ClNO_5$	340.0982
Norketamine	$C_{15}H_{16}ClNO_4$	310.0877
y-Hydroxynorketamine	$C_{15}H_{16}ClNO_5$	326.0826
Compound with Glu and MA		
Ketamine	$C_{22}H_{28}ClNO_9$	486.1525
x-Hydroxyketamine	$C_{22}H_{28}ClNO_{10}$	502.1553
Norketamine	$C_{21}H_{26}ClNO_9$	472.1317
y-Hydroxynorketamine	$C_{21}H_{26}ClNO_{10}$	488.1318

The analysis of ketamine and its conjugates delivered positive results for ketamine and one possible metabolite, namely norketamine, in the root samples. Furthermore, the control window solution confirmed that these compounds are not formed through photochemical reactions or through simple hydrolysis, indicated by their absence in the control solution. Interestingly, no ketamine or metabolites were detected in any of the leaf samples.

The results of the ketamine analysis via the mechanical extraction of the roots are presented in *Table 7*. The peak areas, *A*, and the retention times, *RT*, were taken from the corresponding EICs, depicted in *Figures 16-19.*

To quantify the final concentration in the roots, the peak areas of the sample solutions needed to be adjusted, $A_{adjusted}$, due to the difference in injection volumes between the samples and the standard solutions, with 20 µL and 3 µL, respectively. The ketamine concentration, $\beta_{sol.,}$ in the solution was calculated with the refined calibration curve from *Figure 15* and the adjusted peak

areas from *Table 7*. The weight of the ketamine in the roots, β_{root}, was computed using the extraction volume employed during the analysis (1.5 ml) and the corresponding mass of the initially harvested samples (~ 0.5 g).

Table 7 – Ketamine in garden cress roots; extracted mechanically

Harvest day	**RT / min**	**A / count * s**	**$A_{adjusted}$ / count * s**	**$\beta_{sol.}$ / mg L^{-1}**	**β_{root} / µg g^{-1}**
1	5.6	9579298	1436895	0.1996	0.5922
2	5.6	9204937	1380741	0.1916	0.5796
3	5.6	34135925	5120389	0.7238	2.1693
4	5.6	18804709	2820706	0.3965	1.1889

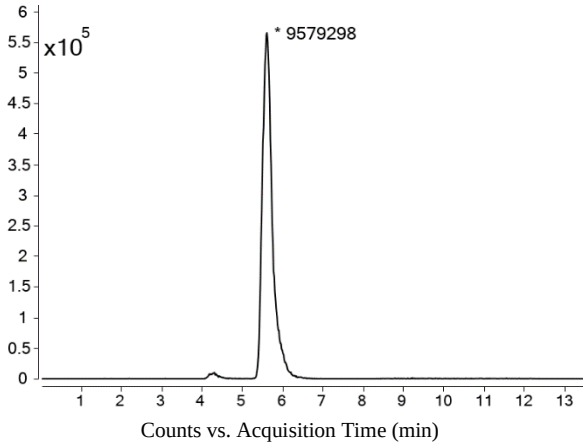

Figure 16 – EIC of ketamine in roots, **harvest day 1**

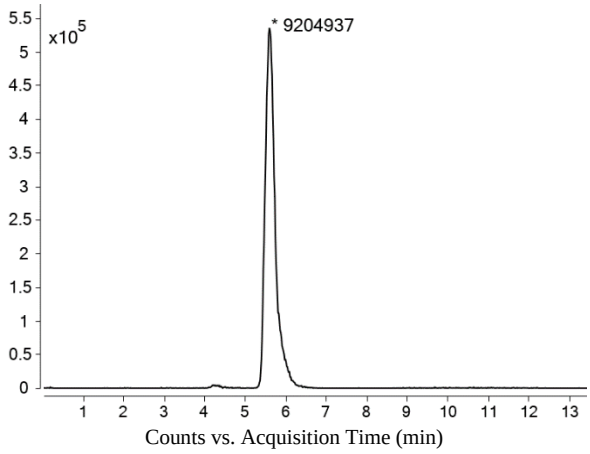

Figure 17 – EIC of ketamine in roots, **harvest day 2**

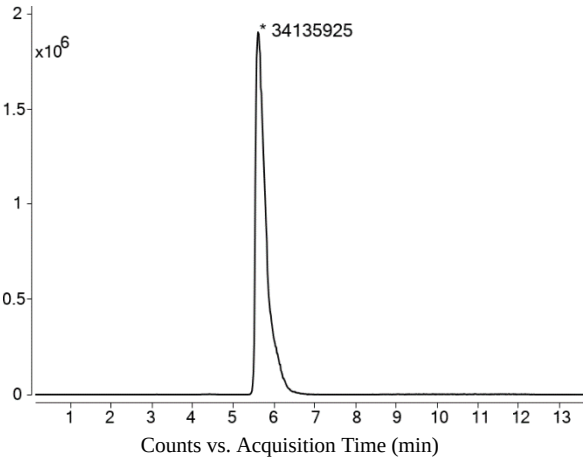

Figure 18 – EIC of ketamine in roots, **harvest day 3**

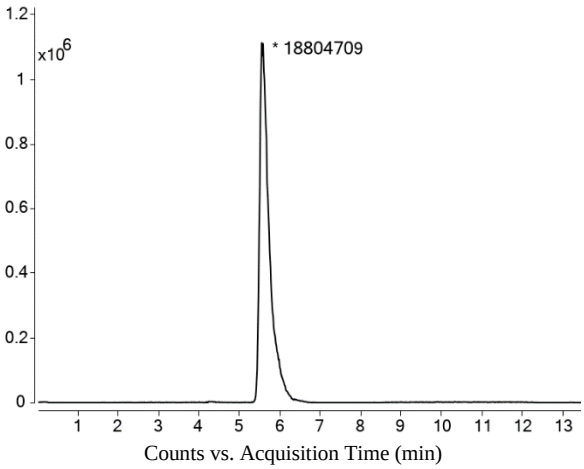

Figure 19 – EIC of ketamine in roots, **harvest day 4**

4.1.1 Ketamine metabolite

The metabolite norketamine (m/z ($[M+H]^+$) = 224.0837) was tentatively identified in the roots of the garden cress. A significant peak with a retention time of 5.0 minutes *(Figure 20)* was detected in all the root samples, with the exception of the root sample from harvest day one. Additionally, this compound eluted before the known ketamine peak, which had a retention time of 5.6 minutes. The lower retention time indicates that this molecule is more polar than ketamine, which correlates with the known polarity differences between norketamine and ketamine.

To examine the identity of the peak, the isotopic pattern in the samples from harvest day three was analysed *(Figure 21)*. As ketamine and norketamine both contain a chlorine heteroatom, the found characteristic isotopic patterns [24] supported the assumption that the peak indeed belongs to norketamine.

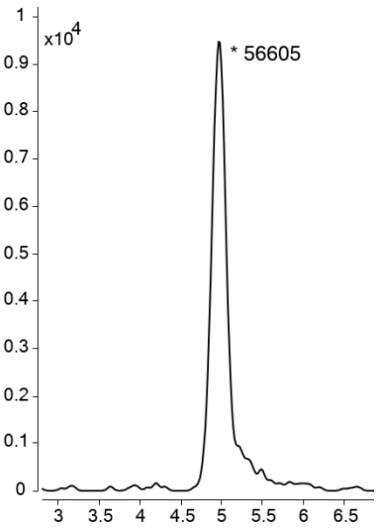

Figure 20 – Tentative **metabolite peak** in the roots

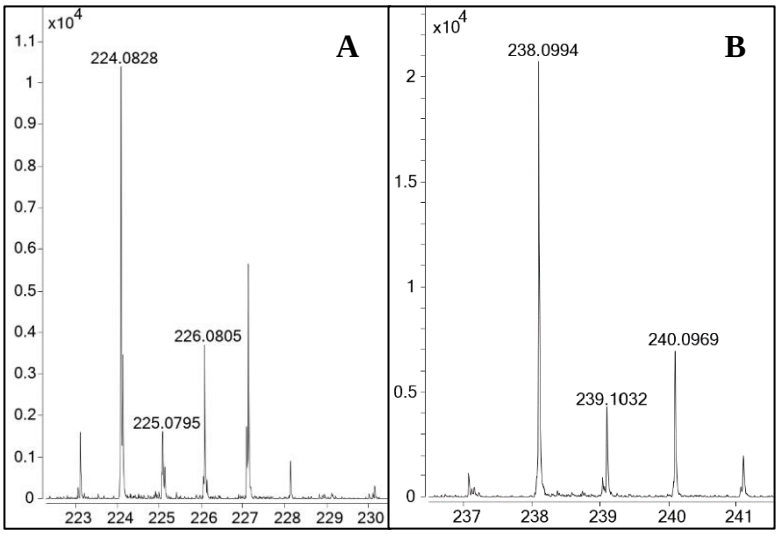

Figure 21 – **Isotopic pattern** of **norketamine** (A) and **ketamine** (B) showing the chlorine characteristic M+2 signal in the roots, from harvest day 3

4.2 Paracetamol

The external calibration curve, shown in *Figure 22*, was created using the EICs of the paracetamol standard solutions *(Figure 23-26)*. These EICs were labelled with the corresponding peak areas, marked with an asterisk. The protonated analyte with an m/z value of 152.0706 eluted at 2.9 minutes. The standard solution with the lowest concentration of 0.001 mg L^{-1} delivered non-interpretable results due to a possible lower signal than the detection limit, and the 100 mg L^{-1} solution again was not measured. Therefore, these two concentrations were not included in the curve.

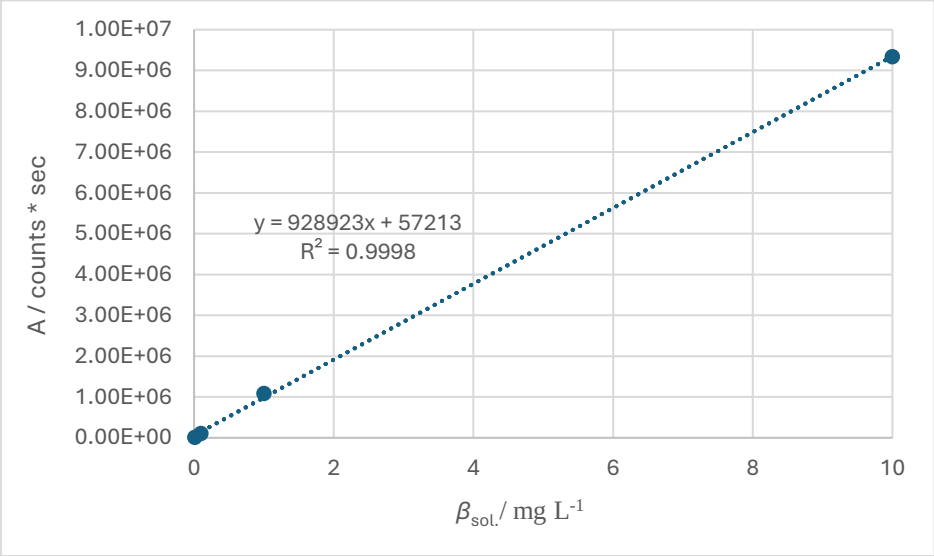

Figure 22 – External calibration curve of paracetamol, with **all** possible **concentrations** included

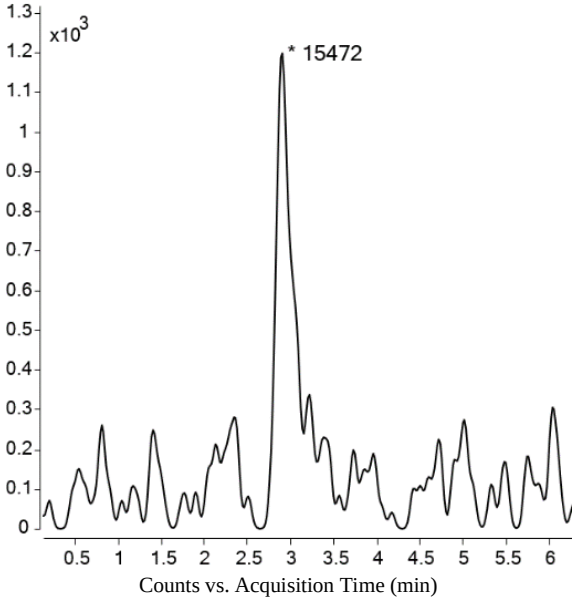

Figure 23 - EIC of **0.01 mg L^{-1}** paracetamol

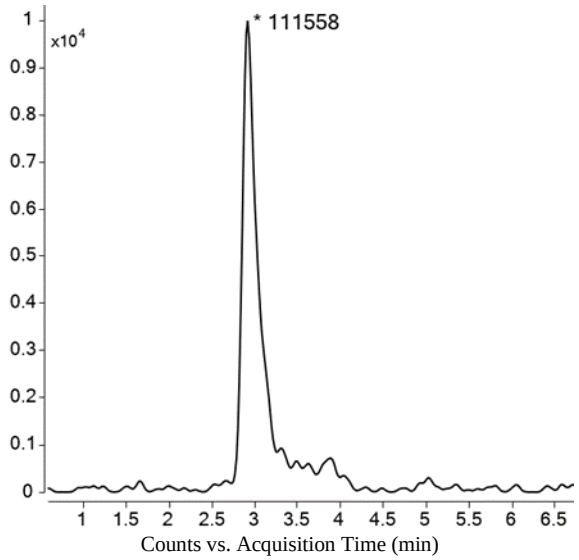

Figure 24 - EIC of **0.1 mg L^{-1}** paracetamol

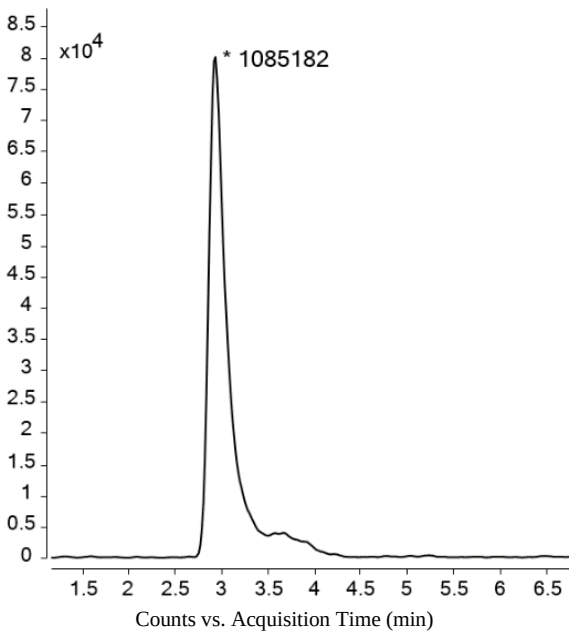

Figure 25 - EIC of **1 mg L^{-1}** paracetamol

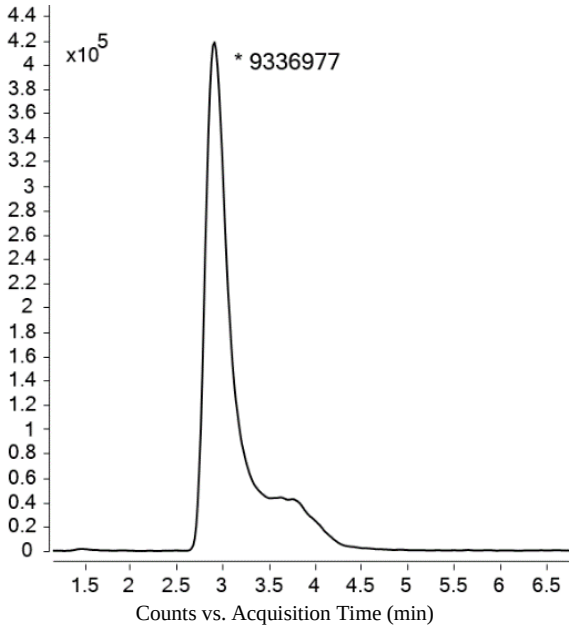

Figure 26 - EIC of **10 mg L^{-1}** paracetamol

The external calibration curve from *Figure 22* was replotted for more accurate results by removing the highest concentration because none of the sample solutions exceeded the peak area belonging to the 1 mg L^{-1} solution. The final external calibration curve and the corresponding equation are depicted in *Figure 27.*

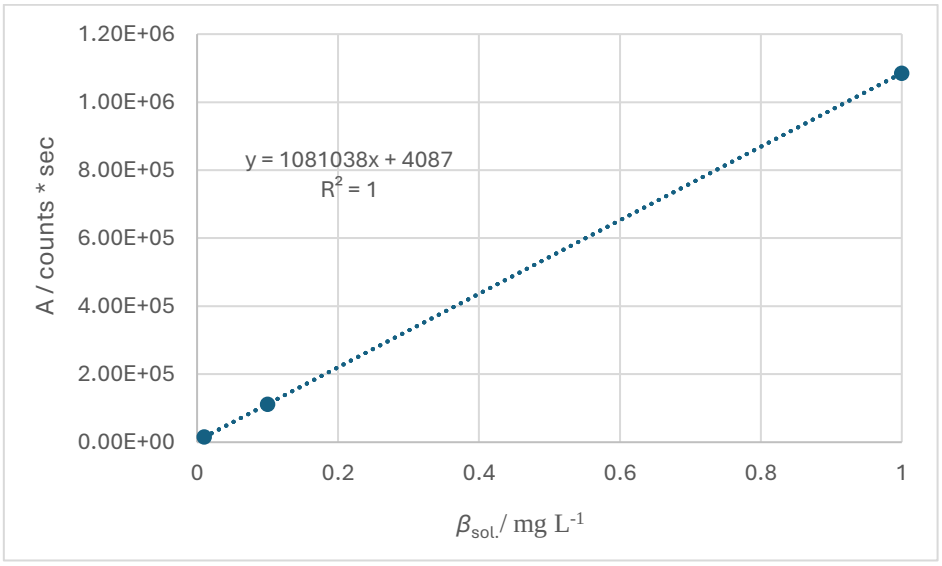

Figure 27 – External calibration curve of paracetamol, in the range of **0.01 – 1 mg L^{-1}**

The EICs of the sample solutions were analysed for the presence of paracetamol, its metabolites as depicted in *Figure 2*, and potential conjugates involving MA, Glu, or both. The summary of all the examined compounds, including the m/z values of their protonated forms, is presented in *Table 8*.

Table 8 – Chemical formulas and the m/z values of the protonated paracetamol metabolites, conjugates

Compound	**Chemical formula**	**m/z ($[M+H]^+$)**
Paracetamol	$C_8H_9NO_2$	152.0706
NAPQI	$C_8H_7NO_2$	150.0550
Acetaminophen sulfate	$C_8H_9NO_5S$	232.0274
Acetaminophen glucuronide	$C_{14}H_{17}NO_8$	328.1207
Acetaminophen cysteine	$C_{11}H_{14}N_2O_3S$	255.0798
Compound with Glu		
Paracetamol	$C_{14}H_{19}NO_7$	314.1234
NAPQI	$C_{14}H_{17}NO_7$	312.1078
Acetaminophen sulfate	$C_{14}H_{19}NO_{10}S$	394.0802
Acetaminophen glucuronide	$C_{20}H_{27}NO_{13}$	490.1579
Acetaminophen cysteine	$C_{17}H_{24}N_2O_8S$	417.1326
Compound with MA		
Paracetamol	$C_{11}H_{11}NO_5$	238.0710
NAPQI	C_{11} H_9NO_5	236.0553
Acetaminophen sulfate	$C_{11}H_{11}NO_8S$	318.0278
Acetaminophen glucuronide	$C_{17}H_{19}NO_{11}$	414.1031
Acetaminophen cysteine	$C_{14}H_{16}N_2O_6S$	341.0802
Compound with Glu and MA		
Paracetamol	$C_{17}H_{21}NO_{10}$	400.1238
NAPQI	$C_{17}H_{19}NO_{10}$	398.1082
Acetaminophen sulfate	$C_{17}H_{21}NO_{13}S$	480.0806
Acetaminophen glucuronide	$C_{23}H_{29}NO_{16}$	576.1583
Acetaminophen cysteine	$C_{20}H_{26}N_2O_{11}S$	503.1330

The analysis confirmed the presence of paracetamol in the root samples; however, it was not detected in the leaves. Metabolites were not found in either of the samples nor in the control window solution.

To quantify paracetamol in the extracted root samples, their peak areas needed to be adjusted, $A_{adjusted}$, due to the difference in injection volumes between the standard and the sample solutions, with 3 µL and 20 µL, respectively. The weight of the paracetamol in the roots, β_{root}, was calculated using the extraction solution volume (1.5 ml) and the corresponding mass of the initially harvested root samples (~ 0.5 g). The results of the mechanically extracted roots

are summarised in *Table 9*. The peak areas, *A*, and retention times, *RT*, were based on the EICs from *Figures* 28 and *29*. The paracetamol concentration in the solution, $\beta_{sol.,}$ was calculated with the calibration curve from *Figure 27* using the adjusted peak areas from *Table 9*. Notably, no paracetamol was detected in the root sample from samples collected on the first and the last harvest days.

Table 9 – Paracetamol in garden cress roots; extracted mechanically

Harvest day	**RT / min**	**A / count * s**	**$A_{adjusted}$ / count * s**	**$\beta_{sol.}$ / mg L^{-1}**	**β_{root} / µg g^{-1}**
2	2.8	797618	119643	0.1069	0.3220
3	2.8	268509	40276	0.0335	0.1008

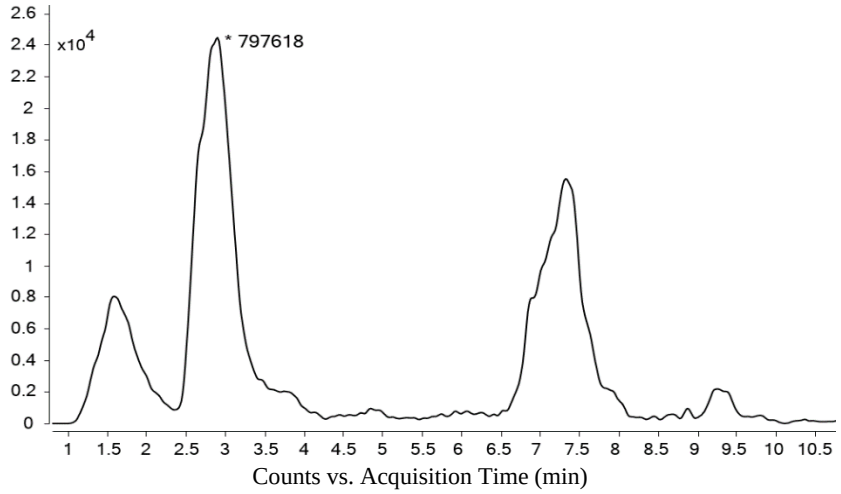

Figure 28 – EIC of paracetamol in roots, **harvest day 2**

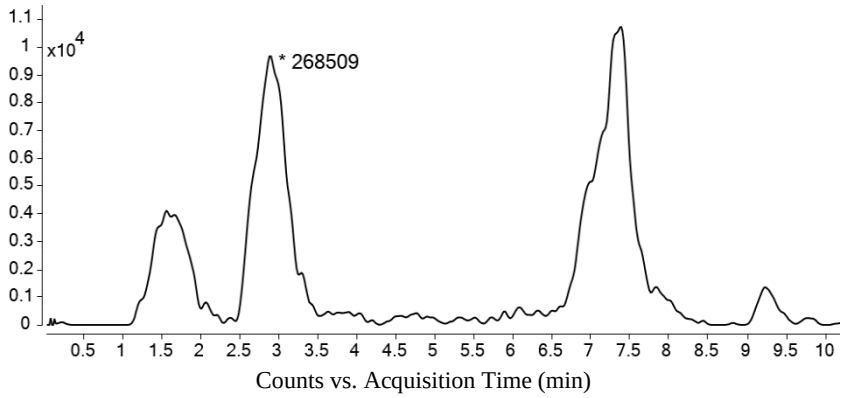

Figure 29 – EIC of paracetamol in roots, **harvest day 3**

4.3 Time study of the API absorption

Figure 30 shows the change in concentration, β_{root}, of the absorbed APIs over time. The pharmaceuticals were predominantly absorbed by the roots, indicated by the absence of paracetamol and ketamine in the leaves, with ketamine being absorbed at significantly higher concentrations than paracetamol. The time study shows that ketamine accumulated over the days, reaching a peak on harvest day three, followed by a considerable decrease. In contrast, the paracetamol concentration had already decreased after harvest day two.

Interestingly, paracetamol was detected only in the root samples collected on harvest days two and three, which may suggest that its concentration fell below the limit of detection in the samples harvested on the other days. The lack of paracetamol on harvest day four could also indicate that by the end of the cultivation period, it had been converted into compounds not targeted by this study.

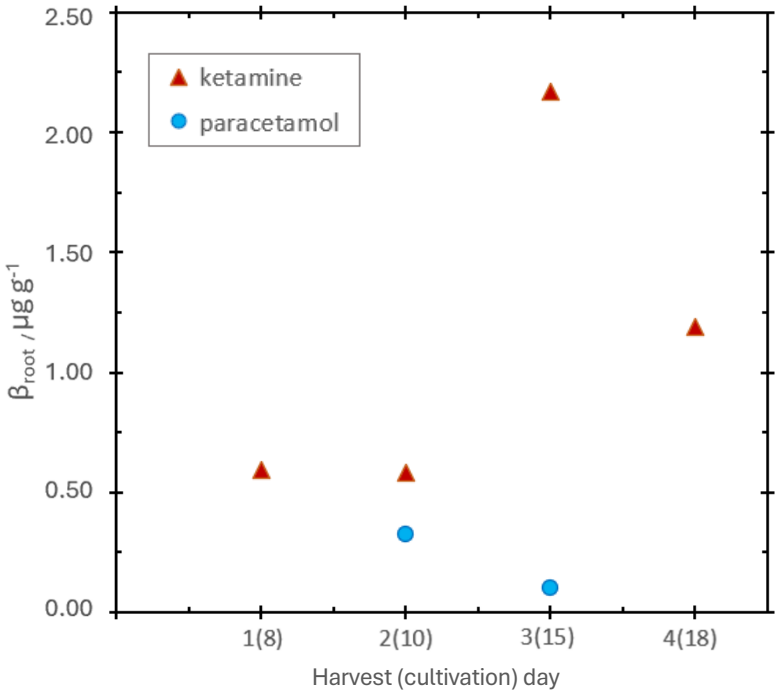

Figure 30 – Time study of the **concentration** of the absorbed APIs

4.4 Manual extraction

To compare manual extraction with the ball grinding extraction method, both paracetamol and ketamine were quantified in roots and leaves that had been extracted using a pestle and a mortar on the second harvest day. Neither of the APIs was detected in the leaf samples. The results are summarised in *Table 10*, and the corresponding EICs are shown in *Figures 31* and *32*.

Table 10 – Ketamine and paracetamol in garden cress roots; extracted manually

Sample	RT / min	A / count * s	$A_{adjusted}$ / count * s	$\beta_{sol.}$ / mg L^{-1}	β_{root} / µg g^{-1}
ketamine	5.6	16824847	2523727	0.3543	1.0562
paracetamol	2.9	8113811	1217072	1.1221	3.3328

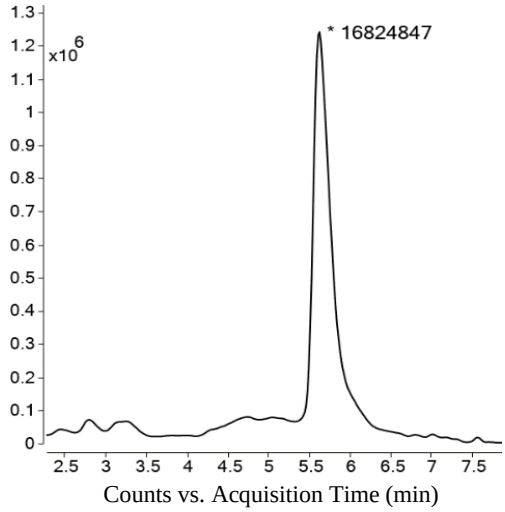

Figure 31 – EIC of **manually** extracted **ketamine** in root

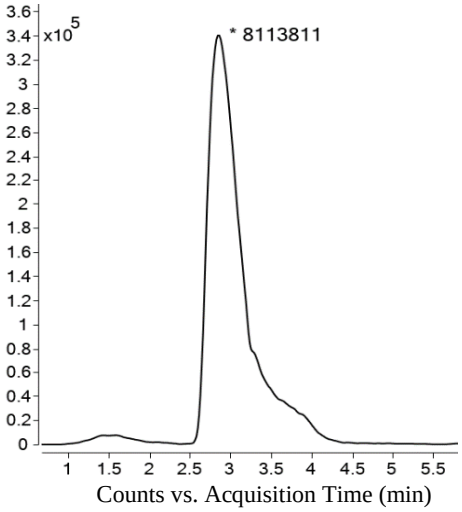

Figure 32 – EIC of **manually** extracted **paracetamol** in root

For a better comparison, *Table 11* summarises the concentrations extracted on the second harvest day using the manual and the mechanical extraction methods. These results indicate that the manual extraction method yields larger concentrations of both ketamine and paracetamol. Especially noticeable is the difference in the extraction methods for paracetamol in roots, where the manual method produced a concentration that was over ten times higher than the one obtained with the mechanical process.

Table 11 – Concentration variation due to different extraction methods

Sample	Mechanical β_{root} / µg g^{-1}	Manual β_{root} / µg g^{-1}
ketamine	0.5796	1.0562
paracetamol	0.3220	3.3328

4.5 MS² fragmentation of parent drug

The MS² fragmentation analysis of the parent compounds, paracetamol and ketamine, was conducted using the standard solutions of 10 mg L^{-1} for both drugs. Root and leaf samples were also fragmented to ensure that the identified compounds in the sample solutions corresponded to the analysed APIs. However, due to the absence of the detectable compounds in the leaf tissues, the fragmentation results from these samples are not included in this analysis.

4.5.1 Ketamine fragmentation

The extracted fragmentation patterns of the ketamine are displayed in the figures below. Specifically, *Figure 33* presents the mass spectrum of the protonated ketamine without fragmentation (m/z ($[M+H]^+$) =~ 238.10), while *Figure 34* shows its complete fragmentation pattern from the 10 mg L^{-1} standard solution. The fragmentation was carried out with different collision energies, ranging from 5 to 20 eV.

As the collision energy increases, there is a noticeable reduction in the signal intensity of the intact molecule, accompanied by the rise in intensity of various lower m/z fragments. The most significant and continuous increase in intensity is observed for the fragment with m/z =~ 125.02. Other critical fragments observed include those with m/z values of approximately 220.09, 207.06, and 179.06. These fragments exhibit a decline in intensity above collision energy of 15 eV, indicating their further breakdown into smaller fragments.

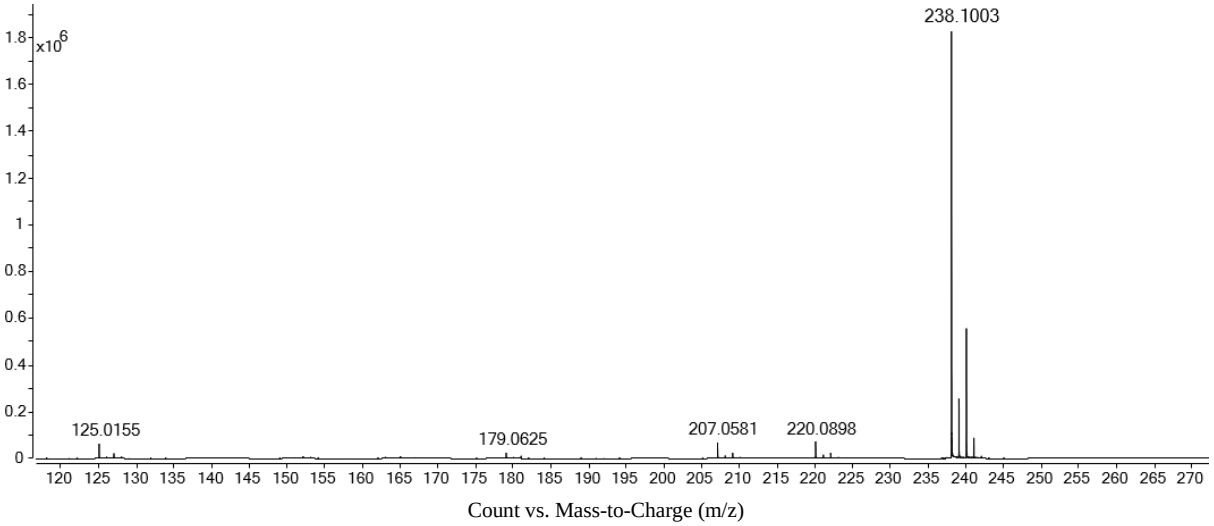

Figure 33 – Mass spectrum of **ketamine** without collision energy

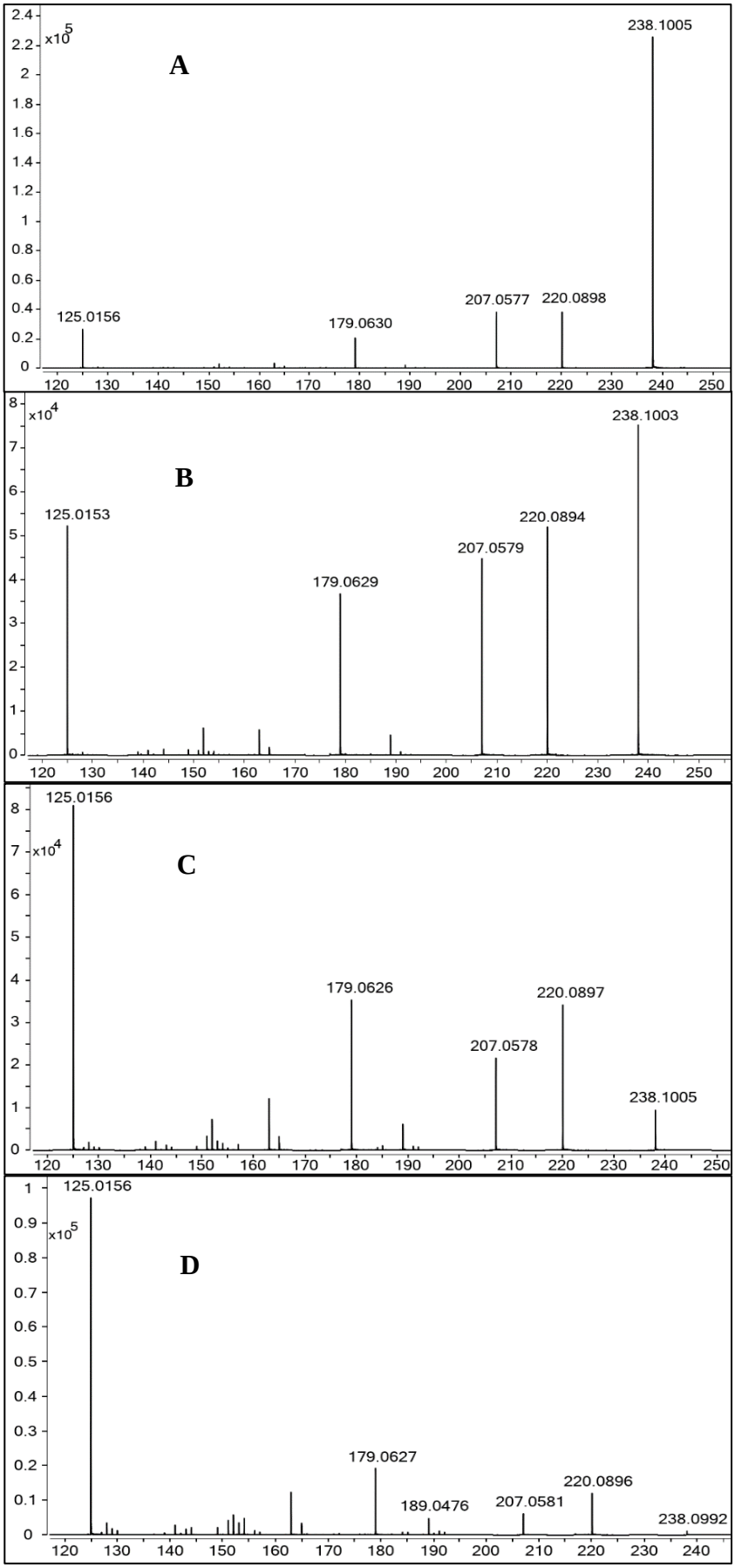

Figure 34 - MS^2 fragmentation of **ketamine** at **5 eV** (A); **10 eV** (B); **15 eV** (C); **20 eV** (D) in the 10 mg L^{-1} **standard solution**

To confirm that the detected analyte in the roots of the garden cress was ketamine, its fragmentation pattern was compared with that of the standard solution. The two MS^2 runs delivered identical patterns, as demonstrated by *Figure 35*, which shows the molecular fragments in the roots at a collision energy of 15 eV. The key fragments with m/z ratios of 125.014, 179.06, 207.06, and 220.087 from *Figure 34/C* are also present in *Figure 35*.

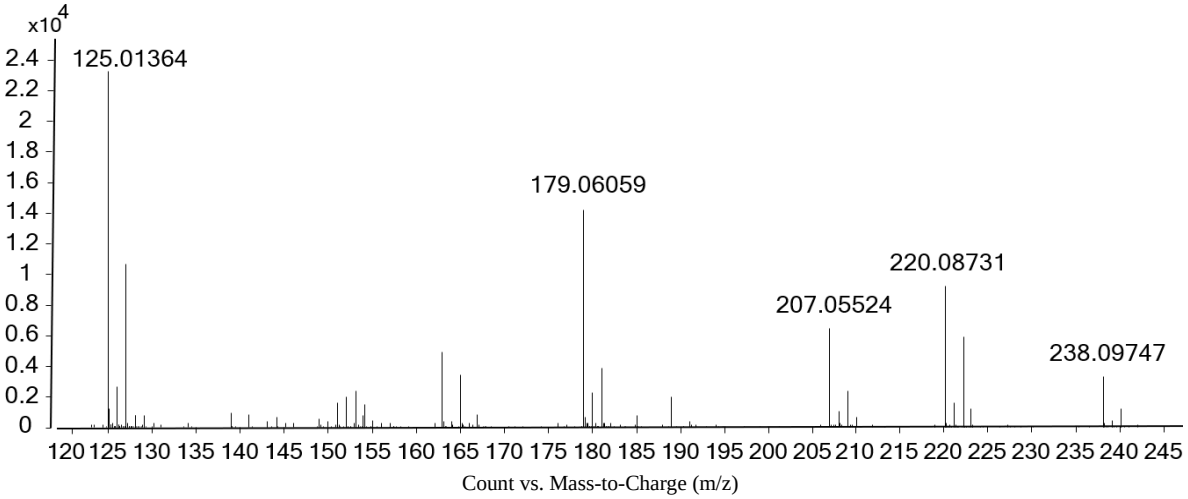

Figure 35 – MS^2 fragmentation of **ketamine** in the **roots**, at a collision energy of **15 eV**

4.5.2 Paracetamol fragmentation

The mass spectrum of protonated paracetamol (m/z ($[M+H]^+$ =~ 152.06) is presented in *Figure 36*, highlighting its molecular ion peak without any fragmentation-inducing collision energy.

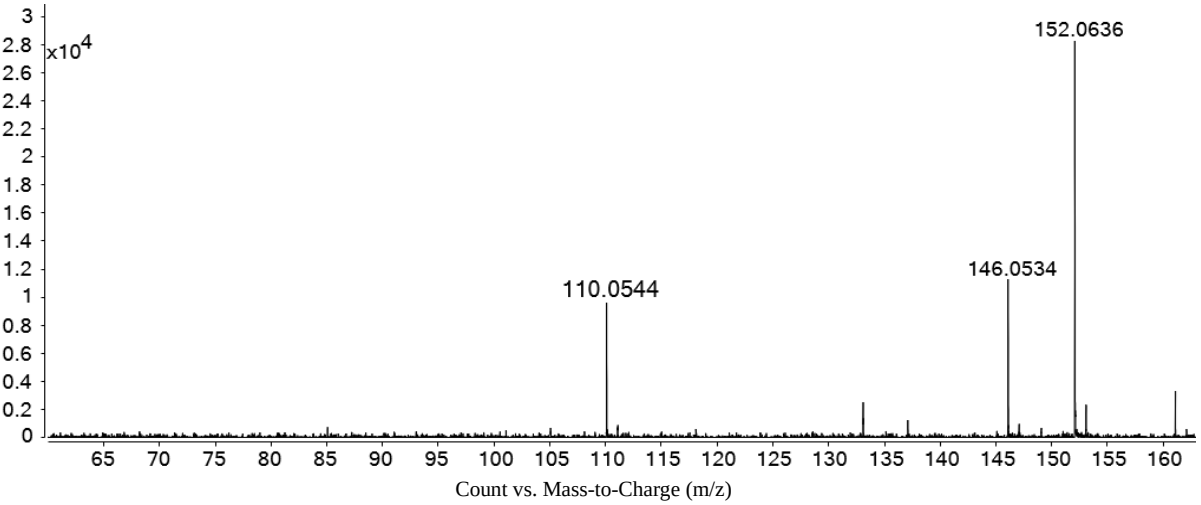

Figure 36 – Mass spectrum of **paracetamol** without collision energy

The distinct fragments of the protonated paracetamol in the range of 5 to 20 eV collision energy are displayed in *Figure 38*. Its fragmentation is indicated by the decreasing intensity of the parent drug peak, coupled with an intensity increase of the other lower m/z fragments. The most significant rise in intensity is seen in the signal with m/z =~ 110.05. At higher collision energies, additional smaller fragments appear, with m/z ratios of approximately 93.03 and 65.03, respectively. At the highest collision energy of 20 eV, the parent drug is entirely fragmented, leading to the complete disappearance of its peak.

To verify the presence of paracetamol in the root samples, its fragmentation pattern was compared with that of the standard solution. The major fragments found were identical, as illustrated by *Figures 37* and *38/C.* These show the MS^2 spectra at 15 eV of the 10 mg L^{-1} standard solution and the root sample from harvest day three.

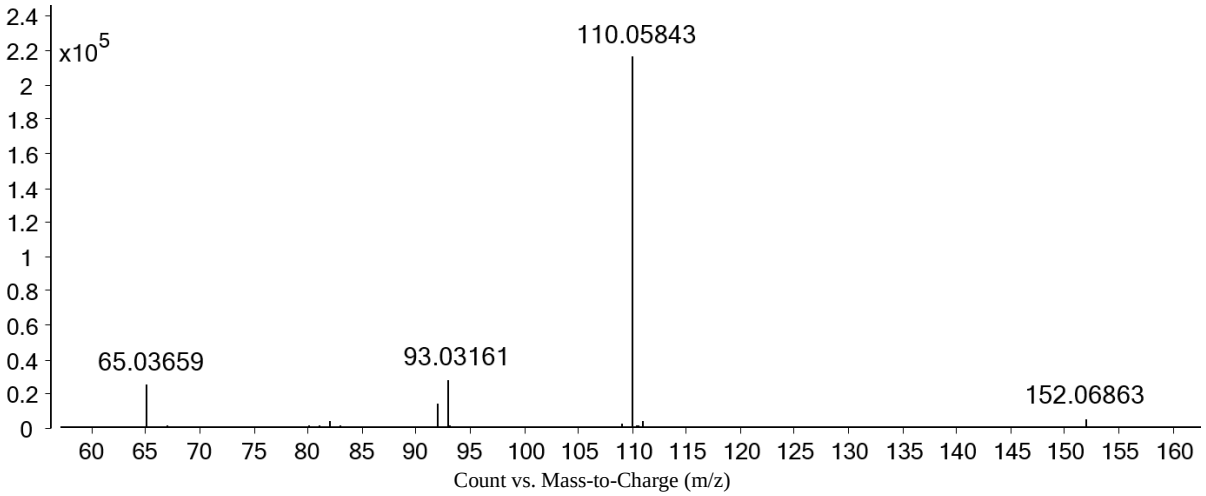

Figure 37 – MS^2 fragmentation of **paracetamol** in the 10 mg L^{-1} **standard solution**, at a collision energy of **15 eV**

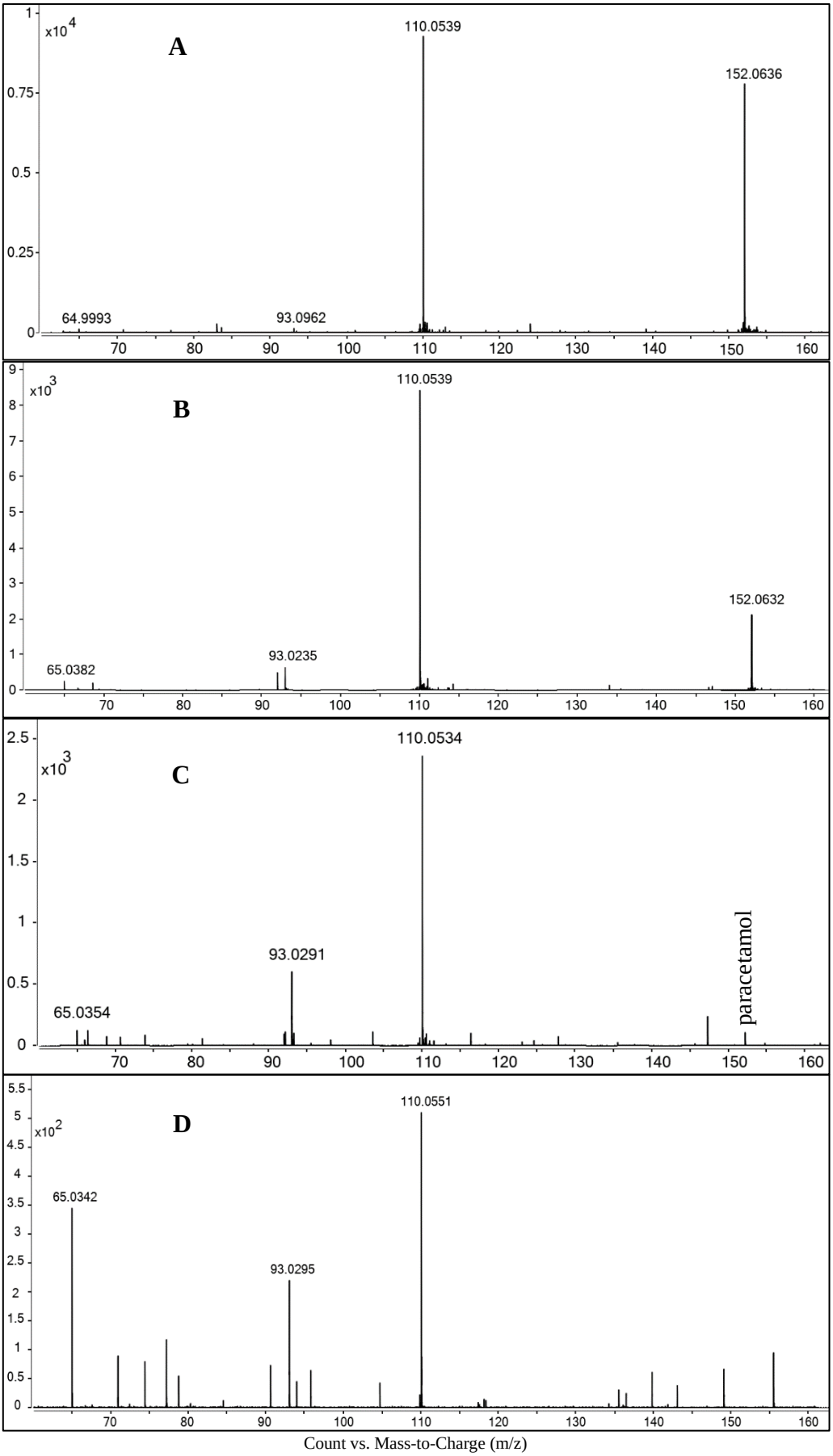

Figure 38 - MS^2 fragmentation of **paracetamol** at **5 eV** (A); **10 eV** (B); **15 eV** (C); **20 eV** (D) in the **roots**

5. Discussion

This study aimed to investigate the uptake of paracetamol and ketamine by garden cress (*Lepidium sativum*) and to compare the effectiveness of two different extraction methods.

In plants, the absorption process in the roots typically occurs through passive diffusion, allowing water and all the dissolved compounds, including organic compounds, to enter. These substances are transferred upwards to the leaves through the xylem via capillary action as part of plants' vascular system [25].

In this research, however, both pharmaceuticals were detected exclusively in the roots at varying rates and concentrations. Ketamine was absorbed by the roots more rapidly and in larger amounts than paracetamol. This is clearly demonstrated by the time study, which revealed that the lowest measured ketamine concentration exceeded the highest measured paracetamol concentration. Given that ketamine was utilised in its highly soluble hydrochloride salt form, these findings support the hypothesis that water solubility is a determining factor in the uptake rate of organic compounds by plants [26].

Despite the rapid and higher uptake of ketamine in the roots, it was not detected in the leaves. One possible explanation is that the exposure time for the ketamine to be translocated to the leaves was insufficient. Another possibility is that ketamine was fully metabolised within the roots; however, this is less likely, considering that the metabolites were absent in the leaves.

The low concentration of paracetamol in the irrigation water used for cultivating the garden cress might explain the minimal amount of paracetamol observed in the roots and its complete absence in the leaves. This assumption aligns with another study, which found that paracetamol uptake depends heavily on its concentration in the irrigation water. In that research, drug-spiked water with ten times the concentration of our study resulted in relatively low paracetamol concentrations in the roots of spinach (*Spinacia oleracea*). Furthermore, they found that the accumulation of paracetamol in spinach leaves was significantly lower compared to when cultivation water with even higher concentrations was used [27].

However, it is important to note that the extraction method used in our study might have also impacted our results. This is supported by the finding that manually ground plant tissues led to substantially higher yields in the collected root than those processed mechanically. The paracetamol concentration was over tenfold higher than that with the mechanical extraction method. Similarly, the manual extraction of ketamine resulted in almost double the

concentration of the ball ground process. Utilising manual extraction and adjusting xenobiotics concentration in the irrigation water might have helped mitigate the potential problem of the analyte concentrations falling below the limit of detection.

Upon investigating the presence of metabolites and conjugates, a tentative metabolite of ketamine, norketamine, was detected in the roots. In contrast, no metabolites or conjugates of paracetamol were found, likely due to the low concentration of paracetamol being insufficient to yield metabolites in detectable concentrations.

To confirm the identity of the potential metabolite peak, the isotopic pattern of the chlorine atom was analysed, as both ketamine and norketamine contain one chlorine atom. Chlorine occurs in two stable isotopes, ^{37}Cl and ^{35}Cl, with natural abundances of 75 % and 25 %, respectively. This creates a unique M + 2 peak in the mass spectrum, with a relative intensity of three to one [28]. These spectral results confirmed chlorine's presence in both the ketamine peak and the peak belonging to the potential metabolite. Moreover, the retention time of the tentative metabolite was lower than the retention time of the ketamine, which indicates this compound is more polar than ketamine itself. Furthermore, the decline in ketamine concentration after harvest day three might be due to its ongoing metabolisation. These findings collectively support the hypothesis that the detected peak is norketamine. However, the definitive conformation of the peak identity would require a fragmentation analysis via tandem mass spectrometry, also known as MS^2.

The same MS^2 verification method successfully confirmed the identity of the primary analytes, ketamine and paracetamol. The fragmentation pattern observed in the mass spectra of the root sample matched those of the standard solutions, providing conclusive evidence that these xenobiotics were indeed present in the roots of the garden cress.

6. Conclusion

This study, with the primary focus on the xenobiotic uptake in garden cress, provides insights into how plants uptake and metabolise exogenous organic compounds. For instance, it was observed that enhanced solubility of a compound can lead to increased absorption by plants. Paracetamol, despite being more polar than ketamine in its commonly used form, was absorbed in smaller amounts than ketamine. This can be attributed to using ketamine in its highly soluble salt form. Additionally, a tentative ketamine metabolite, norketamine, was found in the garden cress roots, confirming its metabolic activity.

Furthermore, this research also explored the effectiveness of two extraction methods. Manually processed root samples yielded significantly higher concentrations than those extracted mechanically. The extraction method employed can enhance the quantification accuracy of the xenobiotics, providing more definitive results.

Given these findings, it is vital to manage the concentration of xenobiotics in wastewater used for irrigation, as these can be taken up by crops, even when present in low concentrations. To prevent their accumulation in consumable plants, these compounds must not exceed safe levels in wastewater employed for irrigation.

References

[1] A. Dai, “Increasing drought under global warming in observations and models,” Nat Clim Chang, vol. 3, no. 1, pp. 52–58, Jan. 2013, doi: 10.1038/nclimate1633.

[2] X. Yang, Y. Pu, S. Weng, M. Hou, and Z. Wang, “Review of agricultural water-saving policies and measures in recent years – a case study of Jiangsu Province, China,” Water Supply, vol. 22, no. 4. IWA Publishing, pp. 3951–3962, Apr. 01, 2022. doi: 10.2166/ws.2022.026.

[3] S. Mishra, R. Kumar, and M. Kumar, “Use of treated sewage or wastewater as an irrigation water for agricultural purposes- Environmental, health, and economic impacts,” Total Environment Research Themes, vol. 6, Jun. 2023, doi: 10.1016/j.totert.2023.100051.

[4] K. S. Karthika, I. Rashmi, and M. S. Parvathi, “Biological functions, uptake and transport of essential nutrients in relation to plant growth,” in Plant Nutrients and Abiotic Stress Tolerance, Springer Singapore, 2018, pp. 1–49. doi: 10.1007/978-981-10-9044-8_1.

[5] T. K. Das and A. Poater, “Review on the use of heavy metal deposits from water treatmentwaste towards catalytic chemical syntheses,” Int J Mol Sci, vol. 22, no. 24, Dec. 2021, doi: 10.3390/ijms222413383.

[6] S. Shojaei, A. Jafarpour, S. Shojaei, Y. Gyasi-Agyei, and J. Rodrigo-Comino, “Heavy metal uptake by plants from wastewater of different pulp concentrations and contaminated soils,” J Clean Prod, vol. 296, May 2021, doi: 10.1016/j.jclepro.2021.126345.

[7] M. J. Abedin, J. Cotter-Howells, and A. A. Meharg, “Arsenic uptake and accumulation in rice (Oryza sativa L.) irrigated with contaminated water,” 2002.

[8] Y. H. Chuang et al., “Mechanistic study on uptake and transport of pharmaceuticals in lettuce from water,” Environ Int, vol. 131, Oct. 2019, doi: 10.1016/j.envint.2019.104976.

[9] D. G. J. Larsson, “Pollution from drug manufacturing: Review and perspectives,” Philosophical Transactions of the Royal Society B: Biological Sciences, vol. 369, no. 1656. Royal Society of London, Nov. 19, 2014. doi: 10.1098/rstb.2013.0571.

[10] C. G. Daughton, T. A. Ternes, C. G. Daughton1, and T. A. Ternes2, “This content downloaded from 195.34.79.223 on Wed,” 1999.

[11] A. Nikolaou, S. Meric, and D. Fatta, “Occurrence patterns of pharmaceuticals in water and wastewater environments,” in Analytical and Bioanalytical Chemistry, Feb. 2007, pp. 1225–1234. doi: 10.1007/s00216-006-1035-8.

[12] J. O. Coleman, M. Blake-Kajff, and T. E. Davies, “Detoxification of xenobiotics by plants: chemical modification and vacuolar compartmentation,” 1997.

[13] C. Warwick, “Paracetamol and fever management,” Journal of The Royal Society for the Promotion of Health, vol. 128, no. 6, pp. 320–323, 2008, doi: 10.1177/1466424008092794.

[14] IARC Working Group on the Evaluation of Carcinogenic Risks to Humans. and International Agency for Research on Cancer., Pharmaceutical drugs. IARC, 1990.

[15] “T3DB, Acetaminophen“. [Online]. http://www.t3db.ca/toxins/T3D2571. [Accessed 14. 06. 2024].

[16] J. G. M. Bessems and N. P. E. Vermeulen, “Paracetamol (Acetaminophen)-Induced Toxicity: Molecular and Biochemical Mechanisms, Analogues and Protective Approaches,” 2001.

[17] “Drug Bank, Acetaminophen“. [Online]. https://go.drugbank.com/drugs/DB00316. [Accessed 14. 06. 2024].

[18] M. Gao, D. Rejaei, and H. Liu, “Ketamine use in current clinical practice,” Acta Pharmacologica Sinica, vol. 37, no. 7. Nature Publishing Group, pp. 865–872, Jul. 01, 2016. doi: 10.1038/aps.2016.5.

[19] H. Trimmel et al., “S(+)-ketamine: Current trends in emergency and intensive care medicine,” Wiener Klinische Wochenschrift, vol. 130, no. 9–10. Springer-Verlag Wien, pp. 356–366, May 01, 2018. doi: 10.1007/s00508-017-1299-3.

[20] A. Nowacka and M. Borczyk, “Ketamine applications beyond anesthesia – A literature review,” Eur J Pharmacol, vol. 860, Oct. 2019, doi: 10.1016/j.ejphar.2019.172547.

[21] “T3DB, Ketamine“ [Online]. http://www.t3db.ca/toxins/T3D3025. [Accessed 14. 06. 2024].

[22] G. Mion and T. Villevieille, “Ketamine Pharmacology: An Update (Pharmacodynamics and Molecular Aspects, Recent Findings),” CNS Neuroscience and Therapeutics, vol. 19, no. 6. pp. 370–380, Jun. 2013. doi: 10.1111/cns.12099.

[23] “Drug Bank, Ketamine“ [Online]. https://go.drugbank.com/drugs/DB01221. [Accessed 14 06. 2024].

[24] Xianming Zhang, Robert A. Di Lorenzo, Paul A. Helm, Eric J. Reiner, Philip H. Howard, Derek C.G. Muir, John G. Sled, Karl J. Jobst, (2019). “Compositional space: A guide for environmental chemists on the identification of persistent and bioaccumulative organics using mass spectrometry.”, Environment International, 104808. doi:10.1016/j.envint.2019.05.002:

[25] McElrone, A. J., Choat, B., Gambetta, G. A. & Brodersen, C. R. (2013) “Water Uptake and Transport in Vascular Plants.” Nature Education Knowledge 4(5):6

[26] Zhang, C., Feng, Y., Liu, Y., Chang, H., Li, Z., & Xue, J. (2017). „Uptake and translocation of organic pollutants in plants: A review.” In *Journal of Integrative Agriculture* (Vol. 16, Issue 8, pp. 1659–1668). Chinese Academy of Agricultural Sciences. https://doi.org/10.1016/S2095-3119(16)61590-3

[27] Badar, Z., Shanableh, A., El-Keblawy, A., Mosa, K. A., Semerjian, L., Mutery, A. al, Hussain, M. I., Bhattacharjee, S., Tsombou, F. M., Ayyaril, S. S., Ahmady, I. M., Elnaggar, A., Mousa, M., & Semreen, M. H. (2022).” Assessment of Uptake, Accumulation and Degradation of Paracetamol in Spinach (Spinacia oleracea L.) under Controlled Laboratory Conditions.” *Plants*, *11*(13). https://doi.org/10.3390/plants11131626

[28] “Mass Spectra - The M+2 Peak” [Online]. https://chemguide.co.uk/analysis/masspec/mplus2.html. [Accessed: 29. 06. 2024]